Detection and Restoration Pipeline for Phase Contrast Microscopy Time Series Images

1st Mahmut UÇAR
Electrical and Electronic Engineering
Izmir Democracy University
İzmir, Turkey
mahmutucar@outlook.com

2nd Leonardo O. IHEME
AI Team
Virasoft Inc.
İstanbul, Turkey
leonardo.iheme@gmail.com

3rd Sevgi ÖNAL
Biotechnology and Bioengineering
Izmir Institute Of Technology
İzmir, Turkey
sevgional1@gmail.com

4,5th Özden Y. ÖZUYSAL, Devrim P. OKVUR
Molecular Biology and Genetics
Izmir Institute Of Technology
İzmir, Turkey
{ozdenyalcin,devrimpesen}@iyte.edu.tr

6th Behçet U. TÖREYİN
Informatics Institute
Istanbul Technical University
Istanbul, Turkey
toreyin@itu.edu.tr

7th Devrim ÜNAY
Electrical and Electronic Engineering
Izmir Democracy University
İzmir, Turkey
unaydevrim@gmail.com

2022 Medical Technologies Congress (TIPTEKNO) | 978-1-6654-5432-2/22/$31.00 ©2022 IEEE | DOI: 10.1109/TIPTEKNO56568.2022.9960161

***Abstract*—We propose a pre-processing pipeline for the detection and restoration of distorted frames in phase-contrast microscopy time-series images. The analysis is based on the average intensity values of the frames within any given time-series image. The extent of the correction of intensity variation in frames is determined by the normalization of the difference between the current frame's average intensity and the median of average intensity of all frames. Our restoration algorithm preserves regional trans-passing pixels, does not cause new distortions, and increases the histogram similarity between the distorted and non-distorted frames. The algorithm was validated on 15,395 time-series image frames from 27 experiments and the results were found to be visually and quantitatively accurate.**

***Index Terms*—pre-processing, detection, restoration, blank-frame, intensity variation, video processing, phase contrast microscopy**

I. Introduction

The pre-processing of data is a crucial step for many studies. When working on deep learning-based (DL) solutions, for instance, data pre-processing has been found to be a prerequisite for the success of the proposed technique [1], [2]. Phase Contrast Microscopy (PCM) and its applications has gained popularity in the past few years [3]–[8]. In order to have higher success rates in the downstream pipelines such as DL-based solutions [9] and conventional machine learning-based (ML) solutions [10], a pre-processing pipeline which, includes the correction of multiple distortions is necessary.

Histogram equalization (HE) and adaptive histogram equalization (AHE) methods are commonly used for image enhancement, however; phase-contrast microscopy images (PCMI) are not using all gray level intensities. Because of that reason when HE or AHE is used, non-distorted frames will also be altered. Contrast limited adaptive histogram equalization (CLAHE) is a more suitable method than HE or AHE for PCMI data. [11] compared the HE, AHE, and CLAHE methods and showed that the CLAHE method displays blood vessels more clearly than HE and AHE. However, CLAHE also produces more noise. As a result, median filtering is applied as a post-processing step after CLAHE. [12] proposed a method that removes flickering from videos. The proposed de-flickering method is effective on sudden and even small amounts of intensity changes. Even though it seemed applicable to our problem, it requires high frame-rate videos as input so that it compares intensity changes of pixels in local areas. The videos in our data set are in AVI format with 20 frames-per-second, where frames are acquired at every 15-minutes during an experiment. Another difference is that the proposed method of [12] exploits local intensity variation, while in our data intensity variations affect the whole frame. [13] suggested a physical correction method for intensity non-uniformity in magnetic resonance images, while [14]–[16] suggested computational solutions for the correction of intensity inhomogeneity in MRI. [17] proposed a segmentation method with inhomogeneous intensity correction on US B-node images.

Although MRIs, ultrasound images, and PCMIs possess a common property of having contiguous z-stacked gray-scale images, such proposed methods are based on non-uniformity of the intensity distribution. PCMI mostly possesses uniform intensity separation in the background for both distorted and non-distorted frames, the variation in intensities of pixels is very little, all pixels are on a very narrow part of the separation interval for non-distorted frames. The physical correction method was suggested for local intensity correction, but we seek a global (whole frame) intensity correction.

On a similar account, non-uniformity correction (NUC) is a common image-enhancement task to adjust for infra-red detector drifts occuring as the scene or the environment change

This work is supported by the Scientific and Technological Research Council of Turkey (TUBITAK) under grant no 119E578.
The data used in this study is collected under the Marie Curie IRG grant (no: FP7 PIRG08-GA-2010-27697).

[18]. Weighted average of neighbouring frames method has more computational work than proposed median thresholding algorithm. Our goal is not the best fit with subsequent frames, Fig. 2-c is showing that best fitting histogram is causing new noises, which will be explained in Section III.

In this study, we propose a new pipeline that takes a video (PCM time-series images) as input, produces relevant quality-related metrics and corrects the detected distorted frames of the video. The proposed pipeline currently detects and corrects blank-frames and frames with intensity variation, respectively.

The paper is organized as follows. Section II explains the acquisition and annotation details of the PCM data used, Section III introduces our proposed detection and restoration solutions for the blank-frame and intensity variation distortions present in PCM data, Section IV presents the results of our proposed solutions, and finally Section V summarizes the conclusions drawn.

II. Data

The data used in our experiments was obtained from the Izmir Institute of Technology Molecular Biology and Genetics Department. It consists of 27 PCM assays of cell motility. In this study, we have focused on detecting and correcting two types of distortions namely: blank frames and intensity variations. Visual examples of the distortions can be seen here and here, respectively.

Two sets of ground truth classifications were made by experts: 1) Video-level classification was performed by watching a video and classifying it based on the type of distortion that was present in it. 2) Frame-level classification was performed by visually examining every frame of a video using the ImageJ software[1] and classifying them based on the type of distortion that was present. For monotonic decreasing of intensity distortion, frame-level ground truth is not prepared.

III. Methods

Our study focuses on the detection and correction of blank frames and intensity variations that are commonly observed in Z-PCM images. A blank frame is a problem for cell tracking algorithms because, on such screens there are no cells to detect. As a result, tracking algorithms could miss the path of the cells that are being tracked. Intensity variations pose a problem to segmentation algorithms as unusual intensity changes between ROIs could lead to the extraction of inconsistent or unrepresentative features. Our restoration algorithm is built on the assumption that the pixel intensity distribution of a given frame is half-normal [19]. Then, we ensure the distribution does not have a long tail. The flowchart of our proposed method is shown in Fig. 1.

In our dataset, there are blank frames resulting from errors during data collection at the laboratory and those that were added synthetically for the purpose of analyses. Regardless of the reason for the presence of blank frames in videos, they are detrimental to downstream processes like cell segmentation and cell tracking. Some videos exhibit an abrupt change in intensity between adjacent frames. While the source of such an artifact is not certain, experts confirm that it results from an unintentionally altered brightness of the light source.

The steps taken to detect and eliminate blank frames are as follows:

- Read the data as a video.
- Average frame intensity (AFI) is calculated for every frame.
- AFI values are floored.
- Save the floored AFI values as a vector in chronological frame order.
- Threshold the AFI vector (‘1’ if vector(i) == 0, else ‘0’).
- Discard frames labeled ‘1’.

After eliminating the blank frames, the algorithm continues as:

- Compute the median of AFI vector.
- Create normalized standard deviation vector
- Threshold the AFI vector at k times the calculated median (the value of k was empirically chosen).
- Frames labeled with ‘1’ have intensity variation problem, while those labeled ‘0’ do not.

To determine a *good* value for k, five videos from our data set were analyzed and 0.3 was chosen empirically as an optimum value. It means that intensity variations that are greater than 30% of the adjacent frames’ average intensity, will be flagged. After the detection step is completed, the restoration algorithm is triggered. It takes the video and the detection results as inputs.

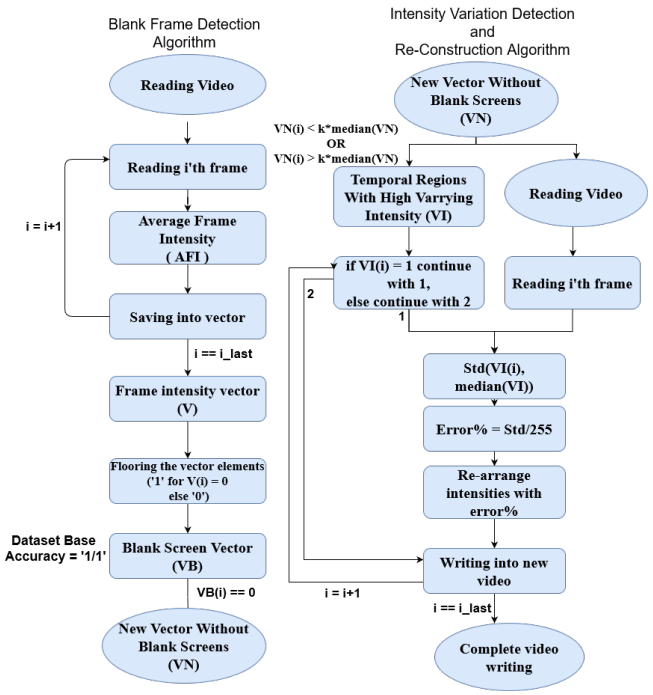

Fig. 1. Flowcharts of our proposed blank frame detection and intensity variation correction algorithms

[1]https://imagej.nih.gov/ij/

PCMI histograms occupy only a narrow band of the 8-bit intensity range. When an intensity variation occurs, the histogram distribution tends to occupy a larger band. To investigate if we could restore distorted frames from the histograms of non-distorted frames, a histogram matching algorithm (HM) was applied. The inputs to the HM algorithm were the distorted frame and the frame which gave the median value of the AFI vector, Fig. 2-c. However, the HM algorithm produced further distortions including:

- Salt noise at the center of the frame
- Very high intensities at the center of cells
- Regional intensity changes

To overcome these short-comings of HM, we designed an algorithm that: 1) preserves regional intensity changes; 2) does not introduce undesired noise; and 3) produces a histogram similar to that of the non-distorted frame.

We compute the normalized standard deviation (σ^n) of the distorted frame. σ^n expresses the difference between the current frame's average intensity and the median AFI. We had chosen median instead of mean value of AFI of frames. Selecting mean value is making algorithm more sensitive to the frames' intensity variation, selecting median value makes the algorithm robust to variations. Equation 1 results in a restored frame in which every pixel is altered by a fixed percentage. Since the pixel values are altered in a frame-by-frame manner, the AFI changes but the regional trans-passing information of the PCMI is preserved.

$$K = \lfloor I * (1 - \sigma^n) \rfloor \tag{1}$$

where I is the current frame, σ^n is the normalized standard deviation and K is the output of Equation 1.

After the application of Equation 1, the resulting frame showed a drastic reduction of pixel intensities. This result was undesirable thus, Equation 1 was modified. Equation 2, similar to 1, preserves the regional trans-passing pixels and reduces the pixel intensities with a fixed percentage. Equation 3 changes the pixel intensities arithmetically. Finally we take the mean of equations 2 and 3 to get 4. The results of equation 4 can be observed in Fig. 2b.

$$L = \lfloor I * \frac{\sigma_i^n}{100} \rfloor \tag{2}$$

$$M = I + J * \frac{\sigma_i^n}{100} \tag{3}$$

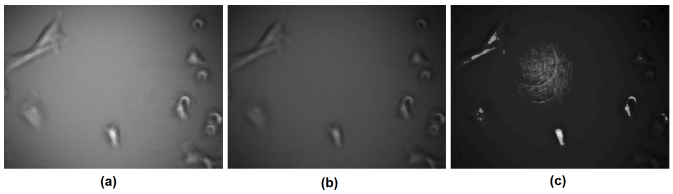

Fig. 2. A distorted frame (a), output of the proposed intensity restoration algorithm applied on the distorted frame (b), output of the conventional histogram matching applied on the distorted frame (c).

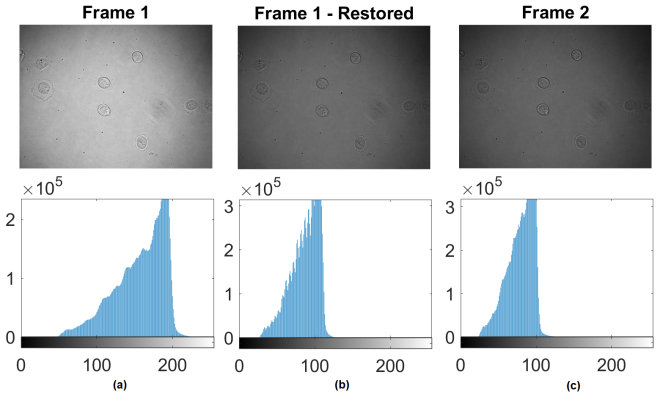

Fig. 3. Distorted frame and its histogram (column a), output of the proposed intensity restoration algorithm applied on the distorted frame and its histogram (column b), and the next non-distorted frame and its histogram (column c).

$$ReconsFrame = \frac{\mathrm{L} + \mathrm{M}}{2} \tag{4}$$

where, σ_i^n refers to the i^{th} element of the normalized standard deviation, σ^n. J is a matrix of ones with the same size as I, L is ouput of Equation 2, M is output of Equation 3 and *ReconsFrame* is the output of Equation 4.

Fig. 3 shows a sample distorted frame, its restored version using our proposed method, and a consecutive non-distorted frame along with their corresponding histograms. As can be seen, the distorted frame has a histogram that covers a larger band of the 8-bit spectrum than the non-distorted frame.

In this study, to evaluate the distortion detection performances of our proposed algorithms we employed the following conventional performance metrics: true positive (TP), false positive (FP), true negative (TN), false negative (FN), and accuracy ($\frac{TP+TN}{TP+TN+FP+FN}$), sensitivity ($\frac{TP}{TP+FN}$), and specificity ($\frac{TN}{TN+FP}$) scores derived from them. Here, a positive item refers to a distorted frame and a true negative corresponds to a non-distorted frame that is correctly identified by the algorithm. Performances are measured at frame-level by considering each frame individually, and video-level by flagging a video as non-distorted if it does not contain any distorted frame.

IV. Results

We evaluated the performance of our detection algorithms for blank-frame and intensity variation problems on the PCM dataset described in Section II, both at frame- and video-levels. Blank-frame detection results presented in Table I and Table II indicate that our algorithm successfully detects all blank frames without any false alarms. It should be noted that the PCM data set is an imbalanced one. Only 164 out of 15,395 frames have blank-frame distortion, while 446 of the 15,395 frames have intensity variation distortion. Hence, total distorted frame rate for our dataset is 0.04%. The proposed method is robust to the inherent imbalance in the data set.

As for the intensity variation, our proposed algorithm produces visually more pleasing results than the conventional HM

TABLE I
VIDEO AND FRAME LEVEL BLANK-FRAME DETECTION PERFORMANCES OF OUR PROPOSED ALGORITHM.

	Video level	Frame level
Accuracy	1.00	1.00
Sensitivity	1.00	1.00
Specificity	1.00	1.00

TABLE II
VIDEO AND FRAME LEVEL CONFUSION MATRICES OF OUR PROPOSED BLANK-FRAME DETECTION ALGORITHM.

	TP	FP	TN	FN
Video level detection	5	0	22	0
Frame level detection	164	0	15,231	0

algorithm (Fig 2). Table IV and Table III display the confusion matrices and the detection performances of our algorithm, respectively. The algorithm is highly accurate at video level detection with just 4 FNs as seen in Table IV. Regarding the frame level detections, as discussed in Section II videos with monotonic intensity variation were not labeled at the frame level, while 386 FPs (Table III) belong to such videos.

Overall our proposed algorithm performs restoration of intensity variations in an accurate manner, i.e. it should output a histogram similar to the neighboring non-distorted frame without injecting any additional distortions such as abrupt local intensity variations or noise. As seen in Fig. 3, histogram of the distorted frame becomes similar (narrower in this example) to that of the next non-distorted frame.

V. CONCLUSION

In this study, we proposed a new pre-processing pipeline for the detection and restoration of distorted frames in phase-contrast microscopy time-series images. The distortions we addressed are the blank-frames and the intensity variations across frames, both of which may hinder the performances of segmentation and tracking algorithms. Our proposed methods, evaluated on PCM time-series images of 27 cell motility experiments, showed outstanding performances for the detection of blank-frames and very high accuracies for the detection of intensity variations. While simple exclusion of the blank-frame from the video stream is sufficient for correction of the former distortion, frames with intensity variations should be restored in a lossless manner. To this end, our proposed restoration method for intensity variations correctly balances out the average intensities across frames without distorting in-frame information. As future work, we plan to include geometric and optical distortions in our detection and restoration pipeline.

TABLE III
VIDEO AND FRAME LEVEL INTENSITY VARIATION DETECTION PERFORMANCES OF OUR PROPOSED ALGORITHM.

	Video level	Frame level
Accuracy	0.85	0.97
Sensitivity	0.69	0.93
Specificity	1.00	0.97

TABLE IV
VIDEO AND FRAME LEVEL CONFUSION MATRICES OF OUR PROPOSED INTENSITY VARIATION DETECTION ALGORITHM.

	TP	FP	TN	FN
Video level detection	9	0	14	4
Frame level detection	413	386	14,538	31

REFERENCES

[1] K. K. Pal and K. Sudeep, "Preprocessing for image classification by convolutional neural networks," in *2016 IEEE International Conference on Recent Trends in Electronics, Information & Communication Technology (RTEICT)*. IEEE, 2016, pp. 1778–1781.

[2] Y. A. LeCun, L. Bottou, G. B. Orr, and K.-R. Müller, "Efficient backprop," in *Neural networks: Tricks of the trade*. Springer, 2012, pp. 9–48.

[3] F. Zernike, "Phase contrast, a new method for the microscopic observation of transparent objects," *Physica*, vol. 9, no. 7, pp. 686–698, 1942.

[4] S. Landry, P. L. McGhee, R. J. Girardin, and W. J. Keeler, "Monitoring live cell viability: Comparative study of fluorescence, oblique incidence reflection and phase contrast microscopy imaging techniques," *Optics express*, vol. 12, no. 23, pp. 5754–5759, 2004.

[5] A. Hand, T. Sun, D. Barber, D. Hose, and S. MacNeil, "Automated tracking of migrating cells in phase-contrast video microscopy sequences using image registration," *Journal of microscopy*, vol. 234, no. 1, pp. 62–79, 2009.

[6] N. Jaccard, L. D. Griffin, A. Keser, R. J. Macown, A. Super, F. S. Veraitch, and N. Szita, "Automated method for the rapid and precise estimation of adherent cell culture characteristics from phase contrast microscopy images," *Biotechnology and bioengineering*, vol. 111, no. 3, pp. 504–517, 2014.

[7] F. Xing, Y. Xie, H. Su, F. Liu, and L. Yang, "Deep learning in microscopy image analysis: A survey," *IEEE transactions on neural networks and learning systems*, vol. 29, no. 10, pp. 4550–4568, 2017.

[8] H.-F. Tsai, J. Gajda, T. F. Sloan, A. Rares, and A. Q. Shen, "Usiigaci: Instance-aware cell tracking in stain-free phase contrast microscopy enabled by machine learning," *SoftwareX*, vol. 9, pp. 230–237, 2019.

[9] A. Ayanzadeh, H. O. Yağar, Y. Özuysal, D. P. Okvur, B. U. Töreyin, D. Ünay, and S. Önal, "Cell segmentation of 2d phase-contrast microscopy images with deep learning method," in *2019 Medical Technologies Congress (TIPTEKNO)*, Oct 2019, pp. 1–4.

[10] Y. S. Erdem, Ö. Y. Özuysal, D. P. Okvur, B. U. Töreyin, and D. Ünay, "An image segmentation method for wound healing assay images," *Natural and Applied Sciences Journal*, vol. 4, no. 1, pp. 30–37.

[11] Maison, T. Lestari, and A. Luthfi, "Retinal blood vessel segmentation using gaussian filter," *Journal of Physics: Conference Series*, vol. 1376, no. 1, p. 012023, nov 2019.

[12] C. Li, Z. Chen, B. Sheng, P. Li, and G. He, "Video flickering removal using temporal reconstruction optimization," *Multimedia Tools and Applications*, vol. 79, no. 7, pp. 4661–4679, 2020.

[13] S. Leger, S. Löck, V. Hietschold, R. Haase, H. J. Böhme, and N. Abolmaali, "Physical correction model for automatic correction of intensity non-uniformity in magnetic resonance imaging," *Physics and Imaging in Radiation Oncology*, vol. 4, pp. 32–38, 2017.

[14] U. Vovk, F. Pernus, and B. Likar, "A Review of Methods for Correction of Intensity Inhomogeneity in MRI," *IEEE Transactions on Medical Imaging*, vol. 26, no. 3, pp. 405–421, 2007.

[15] B. Belaroussi, J. Milles, S. Carme, Y. M. Zhu, and H. Benoit-Cattin, "Intensity non-uniformity correction in MRI: Existing methods and their validation," *Medical Image Analysis*, vol. 10, no. 2, pp. 234–246, 2006.

[16] Z. Hou, "A Review on MR Image Intensity Inhomogeneity Correction," *International Journal of Biomedical Imaging*, vol. 2006, pp. 1–11, 2006.

[17] G. Xiao, M. Brady, J. Noble, and Y. Zhang, "Segmentation of ultrasound B-mode images with intensity inhomogeneity correction," *IEEE Transactions on Medical Imaging*, vol. 21, no. 1, pp. 48–57, 2002.

[18] Y. Tendero, S. Landeau, and J. Gilles, "Non-uniformity correction of infrared images by midway equalization," *Image Processing On Line*, vol. 2, pp. 134–146, 07 2012.

[19] "Half-normal distribution," May 2022. [Online]. Available: https://en.wikipedia.org/wiki/Half-normal_distribution